

On the existence and multiplicity of one-dimensional solid particle attractors in time-dependent Rayleigh-Bénard convection

Marcello Lappa

Telespazio, Via Gianturco 31, Napoli 80046, Italy

(Received 11 July 2012; accepted 7 December 2012; published online 9 January 2013)

For the first time evidence is provided that one-dimensional objects formed by the accumulation of tracer particles can emerge in flows of thermogravitational nature (in the region of the space of parameters, in which the so-called OS (oscillatory solution) flow of the Busse balloon represents the dominant secondary mode of convection). Such structures appear as seemingly rigid filaments, rotating without changing their shape. The most interesting (heretofore unseen) feature of such a class of physical attractors is their variety. Indeed, distinct shapes are found for a fixed value of the Rayleigh number depending on parameters accounting for particle inertia and viscous drag. The fascinating “sea” of existing potential paths, their multiplicity and tortuosity are explained according to the granularity of the loci in the physical space where conditions for phase locking between the traveling thermofluid-dynamic disturbance and the “turnover time” of particles in the basic toroidal flow are satisfied. It is shown, in particular, how the observed wealth of geometric objects and related topological features can be linked to a general overarching attractor representing an intrinsic (particle-independent) property of the base velocity field. © 2013 American Institute of Physics. [<http://dx.doi.org/10.1063/1.4773001>]

Although three-dimensional (3D) time-dependent Rayleigh-Bénard (RB) convection has been the subject of a large amount of research, the associated problem related to the spontaneous accumulation (clustering) of solid particles dispersed in the fluid phase has not been similarly graced. Here this topic is investigated by direct numerical solution of the governing flow-field (Navier-Stokes-Boussinesq) equations in combination with a specific particle-tracking method accounting for particle motion under the influence of inertia and viscous drag. Attention is concentrated on a traveling-wave solution, which of RB convection represents a canonical state. It is shown that, if specific conditions are satisfied, particles, initially uniformly spaced in the liquid, are allowed to demix and form “apparently solid threads,” which rotate at an angular velocity equal to the angular frequency of the thermofluid-dynamic disturbance. The fascinating diversity and complexity of resulting shapes (changing according to inertial properties of particles) distinguish the present case from similar phenomena observed previously for Marangoni (thermocapillary) flow in systems with liquid/gas interfaces. The observed dynamics are explained in the framework of a theory that has its root in a long tradition of past studies devoted to phenomena of inertial particle clustering. This model does not require the presence of a free/liquid gas interface or other intrinsic features of Marangoni convection and is therefore applicable to a vast range of problems and situations.

traced in the phase space having as many dimensions as the number of degrees of freedom of the system.¹ One of the many characteristics of all dissipative systems (systems for which, evolution is driven by competition between a driving force and dissipation of energy) is that their phase trajectories are attracted by a geometric object called “attractor.” This means that different trajectories, arising from different points of the attractor, end on the attractor anyway.

In such a context, much attention has been attracted by Rayleigh-Bénard (RB) convection, which, for the past century, has been the subject of very intensive theoretical, experimental, and numerical studies. Analysis of this kind of flow is of practical importance for many engineering applications and natural phenomena. Even so, the main interest to researchers for this problem is of a theoretical nature as witnessed by the amount of excellent studies appearing in the literature in which Rayleigh-Bénard convection has been used as a paradigm for the study of pattern formation.²⁻⁴

The identification of a “zoo” of possible attractors for this kind of convection is due, in particular, to the landmark research work of Busse,^{5,6} who, focusing on the secondary instabilities which can affect an initial state represented by parallel rolls, determined the boundaries of the region in the space of wavenumber and control parameter where these parallel rolls are stable. It is this line of study that led to the identification of the so-called bimodal, knot and oscillatory (OS) convection (and a variety of other possible spatiotemporal modes appearing in specific regions of the space of parameters, e.g., skewed varicose, cross-roll, ziz-zag, Eckhaus, oscillatory blob convection, etc., for a review see Ref. 7). Other interesting structures are known to be produced in the turbulent state of RB convection by the evolution and clustering in space of thermal plumes originating from instabilities of the wall boundary layers, see, e.g., the excellent

I. INTRODUCTION

The evolution of a dynamical system can be described in general by means of a phase trajectory, which is a curve

investigations by Refs. 8–10 (the reader is also referred to Ref. 11 and all references therein).

Despite the impressive amount of knowledge developed over the years on this subject, the related study of the *clustering dynamics of solid particles suspended in such a kind of flow*, however, seems to be rather limited; indeed, there are no specific results in the literature on the existence and properties of regions behaving as “attractive” loci of points for solid particles in RB flow. This is really surprising if one considers that the general topic related to the ordering and transport of small particles in incompressible flows is of remarkable importance (as well as of general and current interest), as witnessed by important analyses that have been devoted recently to these phenomena (Refs. 12–19). Interestingly, most of these authors were concerned with the direct numerical simulation of homogeneous isotropic turbulence to investigate its interplay with the transport of particles in gases or bubbles in liquids. It was realized that the *inertia* associated with such bubbles or particles can produce preferential concentration of these in regions of instantaneously strong vorticity (for bubbles) or strain-rate (for particles), altering, among other things, the average settling rates and other processes.

Most recently, a parallel line of research has led to the identification of a special class of solid particle attractors in the specific case of Marangoni (thermocapillary) convection (flows that occur if a temperature gradient is imposed along a free liquid/liquid or liquid/gas interface) and for slightly supercritical values of the Marangoni number (“supercritical” here refers to the well-known instability of Marangoni flow that determines transition from an initial axisymmetric steady state to a three-dimensional time-dependent condition characterized by the azimuthal propagation of disturbances, generally known as hydrothermal waves).

The distinguishing feature of this new category of attractors with respect to other incompressible flows is the strictly “one-dimensional nature” (1D) of the structures formed by particle accumulation (despite their peculiar nature, these phenomena are generally simply referred to with the acronym “PAS,” which stands for particle accumulation structures^{20–24}).

This has opened the problem to discern whether the related dynamics can be still explained in the framework of inertial models, like those used to justify the preferential concentration of particles, drops or bubbles in turbulent flows (although not in strictly 1D structures), as discussed above, or other specific non-inertial models (like that elaborated by Ref. 25) have to be necessarily invoked.

Along these lines, the main motivation of the present work is to show that such one-dimensional paths attracting particles in the physical space are neither an exclusive prerogative of Marangoni convection nor an exclusive feature of systems with a free liquid/gas interface, their emergence being possible also in the case of natural flows of gravitational nature (provided specific conditions are established/satisfied).

The problem is investigated resorting to direct numerical solution (DNS) of the Navier-Stokes-Boussinesq equations coupled with solution of the Maxey-Riley equation²⁶ in its simplest form (the so-called inertial equation, derived in the

literature²⁷ as an explicit dissipative equation describing the flow on the slow manifold that governs the asymptotic behavior of inertial particles).

Starting from the cardinal concepts of “inertial segregation”²⁸ and particle spontaneous self-assembly due to “phase locking,”²⁹ in particular, a more spatial approach, an application of what is generally regarded as the “vorticity-based perspective” in fluid dynamics, is used here to explain the cause-effect relationships at the basis of the considered phenomena.

II. MATHEMATICAL MODEL AND METHOD OF ANALYSIS

A. The geometry

Since formation of PAS in Marangoni flow has been observed solely in liquid bridges and when the hydrothermal disturbance travels along a preferred direction (the so-called rotating regime, see Ref. 30), starting point of our analysis is represented by analysis of the RB problem a geometry with the same kind of (axial) symmetry (Figure 1).

Moreover, circumstances are considered for which, on the basis of the Busse balloon, the expected secondary mode of Rayleigh-Bénard convection corresponds to the aforementioned (OS) Oscillatory Instability (unlike other modes of the Busse balloon, this instability does not destroy the underlying roll structure and does not create defects; it simply adds a wave that propagates along the rolls^{31–33}).

Accordingly, we focus on the following case: an annulus with internal and external radii $a = L$ and $b = 5L$ (L being the axial extension of the system) delimited by solid horizontal and vertical walls (bottom heated, top cooled and, adiabatic conditions on the two remaining walls). The considered values of the Prandtl and Rayleigh numbers are $Pr = 1$ and $Ra = 3.5 \times 10^4$, respectively ($Pr = \nu/\alpha$, Ra defined as $g\beta_T\Delta TL^3/\nu\alpha$ where g is the gravity acceleration, β_T the thermal expansion coefficient, ΔT the imposed temperature gradient, ν and α the kinematic viscosity and thermal diffusivity, respectively).

B. Nondimensional field equations

The Navier-Stokes-Boussinesq equations are considered in the nondimensional form obtained by scaling the cylindrical coordinates (\bar{r}, \bar{z}) by L and the velocity components in the axial, radial, and azimuthal directions $(\bar{V}_z, \bar{V}_r, \bar{V}_\phi)$ by the energy diffusion velocity $V_\alpha = \alpha/L$ [the scales for time (t), pressure (p),

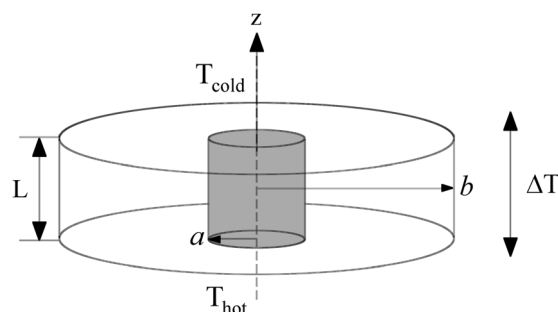


FIG. 1. The *annular domain*, a region having cylindrical symmetry with a cooled top wall, a heated bottom boundary, an inner adiabatic wall (radius a), an outer adiabatic wall (radius b), and depth L .

and temperature (T) being, respectively, L^2/α , $\rho\alpha^2/L^2$ and ΔT , where ρ is the fluid density]. These equations read

$$\underline{\nabla} \cdot \underline{V} = 0, \quad (1)$$

$$\frac{\partial \underline{V}}{\partial t} = -\underline{\nabla} p - \underline{\nabla} \cdot [\underline{V}\underline{V}] + \text{Pr} \nabla^2 \underline{V} - \text{Pr} Ra T \underline{i}_g, \quad (2)$$

$$\frac{\partial T}{\partial t} + \underline{\nabla} \cdot [\underline{V}T] = \nabla^2 T, \quad (3)$$

where \underline{i}_g is the unit vector along the direction of gravity ($\underline{i}_g = -\underline{i}_z$).

C. Boundary conditions

The kinematic conditions to be imposed on the walls simply reflect the well-known no-slip and impermeability properties of solid boundaries ($V_z = V_r = V_\phi = 0$). We do not report them here explicitly for the sake of brevity (and given their extreme simplicity). For problem closure, such conditions, however, have to be supplemented with those for the energy equation. Like usual studies on the subject, the lower ($z=0$) and upper ($z=1$) walls of the domain are assumed here to be at uniform and constant (nondimensional) temperatures $T_0 = 1$ and $T_1 = 0$ respectively, while the vertical walls are adiabatic, i.e., the $\partial T / \partial r = 0$ condition is imposed there.

D. Particle tracking equation

As mentioned in the Introduction, it is a well-known fact (it has been observed both experimentally, and numerically, resorting to the so-called Maxey-Riley equation²⁶) that the dynamics of finite-size particles can differ markedly from infinitesimal particle dynamics. For many applications, however, the complete Maxey-Riley equation is too complex and broad in scope. Rather, obtaining a robust understanding requires a diversity of model types, ranging from simple to complex, in which various processes can be turned on and off and the results carefully diagnosed (this is called a modeling hierarchy and its use forms the backbone of forward progress in any field). Along these lines, a reduction of the equation for particle motion can be considered instrumental in characterizing unambiguously those underlying salient ingredients in the process leading to PAS formation, which are expected to be decisive for other systems/circumstances too.

Since a commonly used *modus operandi* (with a long tradition of past studies on the subject of inertial segregation) is to collapse the particle-motion equation on the slow manifold that governs the asymptotic behavior of inertial particles in the frame of reference rotating at the same angular frequency of the thermofluid-dynamic disturbance,^{28,29} here we undertake the same approach. Accordingly, the particle-tracking equation is cast in compact (nondimensional) form as:

$$\underline{V}_{part} = \underline{V} - \eta \left(\frac{D\underline{V}}{Dt} - \gamma \underline{i}_g \right) + O(St^2), \quad (4)$$

where \underline{V}_{part} is the particle velocity, \underline{V} is the fluid velocity, $\eta = \frac{\tau\alpha}{L^2}(\xi - 1)$, ξ is the ratio of the particle to the fluid density (assumed to be 1.5), τ is the so-called relaxation time,

related to the solid particle radius \tilde{R} by the expression $\tau = \frac{2}{9} \frac{\tilde{R}^2}{\nu}$, and the Stokes number St is defined as $St = \frac{2}{9} \left(\frac{\tilde{R}}{L} \right)^2 \frac{U}{\nu}$, U being the characteristic flow speed ($St \ll 1$ for the conditions considered here). Moreover, $\gamma = \frac{gL^3}{\alpha^2}$ is the term accounting for gravity.

This equation, which can be considered valid when both conditions $\tilde{R}/L \ll 1$ and $U\tilde{R}/\nu \ll 1$ are satisfied, describes the dynamics of small particles dominated by the inertia (including the so-called added mass effect) and viscous drag forces. The centrifugal force, however, is neglected (under the assumption that $\Omega^2 b/g \ll 1$, where Ω is the characteristic particle angular velocity). Moreover, in line with earlier studies,^{25,29} particles are assumed to be independent of each other (hence neglecting any possible mutual interference) and *passive* with respect to the flow (this is the so-called one-way coupling assumption, i.e., no back influence of particles on flow is considered).

E. Solution method and validation study

Balance equations (1)–(3) have been solved numerically in primitive variables by a time-explicit finite-difference method (SMAC method), the domain being discretized with a cylindrical mesh and the flow field variables defined over a staggered grid. Forward differences in time and central-differencing schemes in space (second order accurate) have been used to discretize the energy and momentum partial differential equations. The related algorithm is no longer discussed here. The interested reader is referred for additional details to various books and articles in the literature (for the implementation of this method on parallel machines, the reader may consider, e.g., Refs. 34 and 35).

The present code was successfully used for numerous studies of Marangoni flows and repeatedly validated also by comparison with other kinds of convection (of various natures, see, e.g., Ref. 7).

The above statement, however, does not apply to the part concerning the computation of PAS, for which separate/additional validation has been deemed necessary and for which additional details have to be provided about the specific solution strategy employed.

Towards this end, we may start from the observation that the flow field required at an arbitrary point of the volume (occupied by the generic moving particle) has been linearly interpolated on the computational grid (i.e., linear interpolation of the velocity field has been used for obtaining \underline{V} and the related substantial derivative at the particles' locations).

PAS simulation on the basis of such approach has been then validated by comparison with the numerical results of Melnikov *et al.*,³⁶ who considered Marangoni flow in a liquid bridge with aspect ratio (height/diameter) = 0.34, $\text{Pr} = 8$ (NaNO_3), $\text{Ma} = 20\,600$ (where Ma is defined as $\sigma_T \Delta T L / \mu \alpha$ where ΔT is the applied temperature gradient, μ the dynamic viscosity, and σ_T the surface tension derivative).

Results of the validation study are shown in Table I.

Particles (4×10^3) were seeded into the computational domain initially collected into two perpendicular planes and assumed to be motionless. Fig. 2(a) shows their final location

TABLE I. Comparison with the results of Melnikov *et al.*³⁶

Reference	Grid ($N_z \times N_r \times N_\phi$)	Mode m	Nondimensional angular frequency of the hydrothermal wave $\Omega = 2\pi f/m$	PAS
36	$40 \times 40 \times 32$	3	73.3	Yes
Present	$32 \times 40 \times 40$	3	71.4	Yes

in space with the emergence of the well-known pattern resulting from the accumulation and ordering dynamics.

The value of η considered for this simulation was $\eta = 1 \times 10^{-5}$, which corresponds to particles with size $45 \mu\text{m}$ and solid/fluid density ratio $\xi = 1.85$ considered by Melnikov *et al.*³⁶ Fig. 2(b) illustrates the typical distribution of particles obtained for $\eta = 1 \times 10^{-6}$, which indicates that no PAS are formed unless η is larger than a threshold value. This aspect is of crucial importance in demonstrating the reliability of the present algorithm.

Indeed, it is general consensus that PAS can emerge as numerical “artifacts” (i.e., nonphysical phenomena) if the used algorithm fails in keeping the velocity field solenoidal, i.e., in maintaining the condition $\nabla \cdot \underline{V} = 0$ satisfied with a reasonable approximation and/or if the accuracy of the numerical scheme used for integrating the particle-tracking equation is scarce.

It is obvious, that if PAS were produced by the algorithm as the mere expression of numerical errors, then PAS patterns (as mere artifacts of the numerical simulation) would emerge regardless of the considered value of the inertia parameter η . In particular, if PAS were the outcome of the accumulation of numerical errors related to a non sufficient “volume-preserving” ability of numerical schemes, then one would obtain PAS even in the limit as $\eta \rightarrow 0$. This condition, therefore, can be used as a criterion to discern. Obviously, one must also keep in mind that the other sensitive parameter to be considered in such analysis is the effective time integration step used for the simulations and its influence on the emergence of PAS (indeed, regardless of the order and nature, explicit or implicit, of the integration scheme, the “numerical error” will tend to zero as the time integration step (Δt) goes to zero).

Along these lines, in the present work, the following strategy has been used to guarantee that the emerging PAS are “physical”: assuming no particle inertia, it has been verified

that no PAS patterns are formed using a sufficiently small time integration step Δt (in a sufficiently long time, say 10^2 times the interval required for the formation of physical PAS).

In practice, this criterion is in general implicitly satisfied when the particle-motion equation is integrated together with the 3D Navier-Stokes equations (i.e., at the same time and with the same integration step); indeed, for these equations, the Δt required by the numerical stability of the integration algorithm is very small (several orders of magnitude smaller than that used by other authors who solved the particle-tracking equation “separately,” i.e., resorting to idealized analytical solutions for the base flow or a “frozen” solution of the Navier-Stokes equation assumed to rotate at the same angular frequency of the related thermofluid-dynamic disturbance).

We performed a simulation of particle motion by setting $\eta = 0$ and albeit the very long time simulated (50 times the time required for PAS formation when η is in the right range) no stable or recognizable association of particles was observed (Fig. 2(b)). Rather, emergence of PAS was obtained only when the size of tracers exceeded the same critical size (inertial parameter) identified by Melnikov *et al.*³⁶ (numerical simulations) and Schwabe *et al.*²³ (experiments), which is at the basis of the validation criterion used here. The same philosophy has been used for the simulations of PAS in RB flow (as an example, Figure 3 shows the failure in obtaining particle demixing and ensuing formation of one-dimensional structures for $\eta = 0$).

F. Mesh, scheme order and error analysis

A grid $N_z \times N_r \times N_\phi$: $30 \times 62 \times 90$ (selected on the basis of a grid refinement study assuming convergence when the percentage variation of the maximum of azimuthal velocity becomes less than 3%) has been used for the present simulations of RB convection for the conditions specified in Sec. II A.

As anticipated, in Sec. II E, unlike earlier articles^{25,36} focusing on Marangoni flow, where the particle equation was solved “separately” (the 3D solution was frozen to save computational time and the particle tracking equation solved using such a frozen solution as a “background” state), here Eq. (4) has been dynamically integrated together with Eqs. (1)–(3) (i.e., at the same time and with the same time integration step).

This is an important difference. Given the small value of the nondimensional time integration step Δt required for the

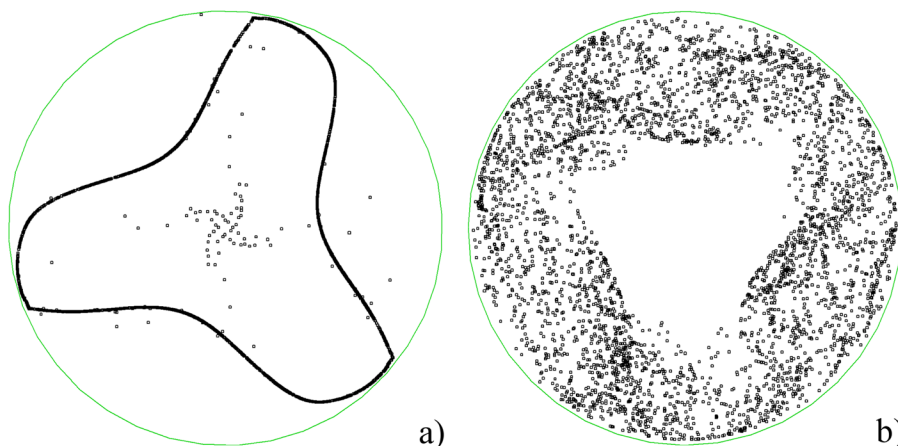


FIG. 2. Projection of spatial particle distribution in the xy plane (liquid bridge of NaNO_3 , $\text{Pr} = 8$, $A = 0.34$, $\text{Ma} = 20\,600$): (a) $\eta = 1 \times 10^{-5}$ (snapshot of PAS at $t = \tau_{\text{PAS}} \cong 2 \times 10^{-1}$); (b) $\eta = 1 \times 10^{-6}$ at $t = 50 \times \tau_{\text{PAS}}$ where $\tau_{\text{PAS}} \cong 2 \times 10^{-1}$ is the nondimensional time required for PAS formation in (a) (in this case no PAS is formed, the same behavior occurs for $\eta = 0$).

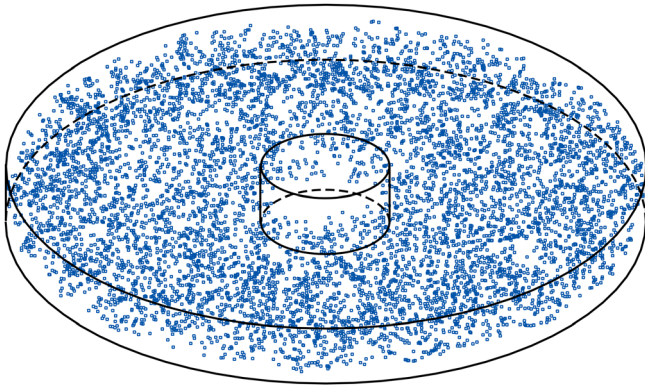


FIG. 3. 3D Snapshot of particle distribution for $Pr = 1$ and $Ra = 3.5 \times 10^4$ in an annulus with internal and external radii $a = L$ and $b = 5L$ (L being the axial extension of the system) in the case of no particle inertia considered ($\eta = 0$, $N_{iter} = 10^7$).

stability of the Navier-Stokes algorithm ($\Delta t \cong 10^{-6}$), one is not forced to use high-order schemes for the integration of Eq. (4). Even with a first-order scheme, in fact, the error produced at each step (the so-called local truncation error³⁷) is $O(\Delta t^2)$, which accumulated over the number of iterations N_{iter} required for PAS formation in the RB case considered here (typically $N_{iter} \cong 2.3 \times 10^6$ as will be discussed in detail in Sec. III), gives a global truncation error³⁷ $N_{iter} \Delta t^2 = O(10^{-6})$.

III. RESULTS

A. The traveling wave state

A snapshot of the thermofluid-dynamic field in the OS state for the considered conditions ($Pr = 1$ and $Ra = 3.5 \times 10^4$) is shown in Fig. 4. Resorting to a spatial perspective, this state can be imagined (such a schematic view will prove very

useful for the description/characterization of related PAS dynamics given later) as the superposition of a series of concentric axisymmetric toroidal rolls (like those existing prior to the onset of timedependent 3D flow, generally referred to as “target patterns” in the context of studies devoted to RB convection) and a disturbance traveling in the azimuthal direction.

In particular, 3 distinct rolls and 10 temperature extremes (disturbances nodes) can be distinguished in the meridian plane and in the cross-section (perpendicular to the symmetry axis), respectively (which indicates that for the considered case the flow is given by a three-roll toroidal structure supporting the propagation of a disturbance with azimuthal wavenumber $m = 10$; the related nondimensional angular frequency, computed as $\Omega = 2\pi f/m$ where f is the frequency of the temperature oscillations measured at a generic mesh point, is $\Omega \cong 5.456$).

B. The properties of the emerging PAS

Snapshots of PAS for distinct values of the inertia parameter η , obtained from N particles ($N = 8 \times 10^3$) arbitrarily seeded into the field are shown in Fig. 5. The related value of the parameter accounting for gravity has been fixed to $\gamma = 10^5$ (this being the limit value “tolerated” by PAS, whose formation is otherwise prevented by particle sedimentation).

As a general feature already discussed for the case of Marangoni flow in Sec. II E, PAS emerge only if η is larger than a threshold value (e.g., no PAS is visible in Fig. 5(a)) as apparently solid structures rotating at the same angular frequency of the thermofluid-dynamic disturbance. Particles initially dispersed in the fluid collect into a seemingly rigid filament that moves as a unit; such a structure is stable and

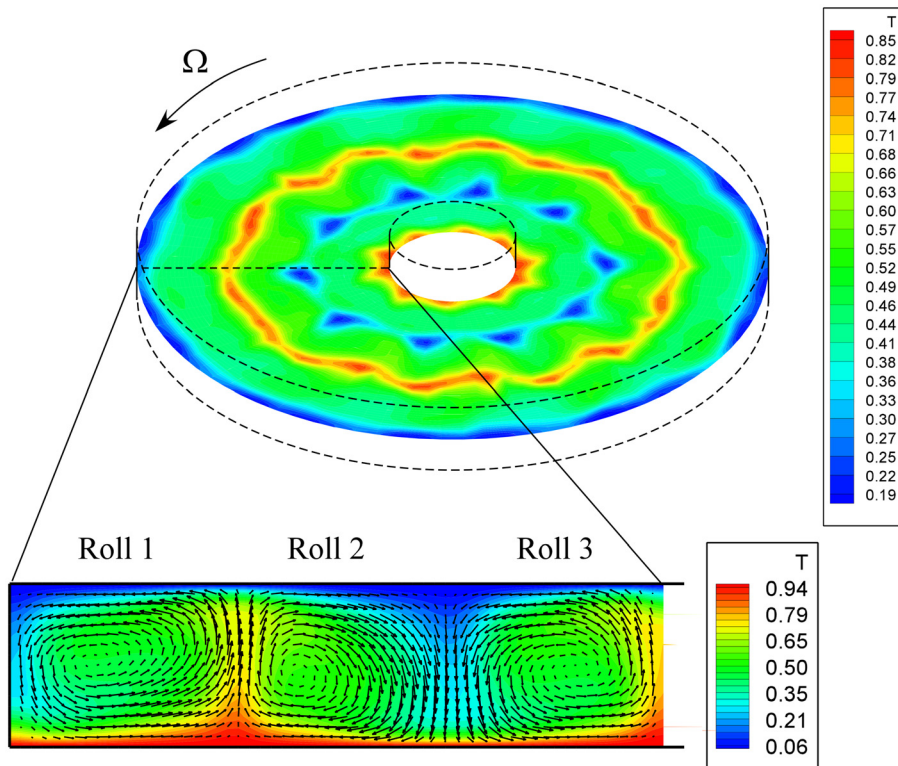


FIG. 4. Snapshot of traveling-wave state of RB convection for $Pr = 1$, and $Ra = 3.5 \times 10^4$ (temperature distribution for $z = 0.5$ and related thermofluid-dynamic field in a meridian section).

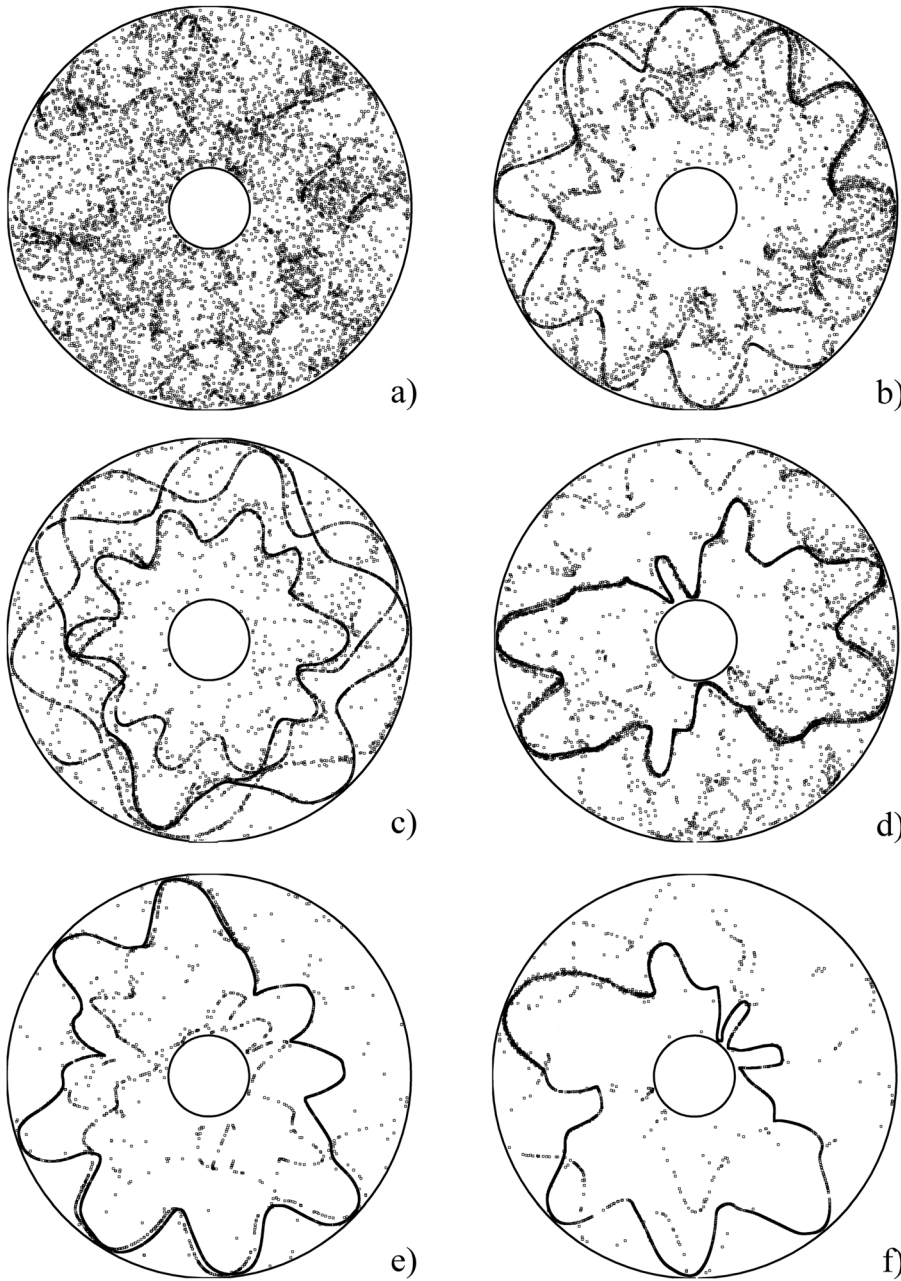


FIG. 5. Snapshots of PAS for different values of the inertia parameter (nondimensional time $= 2 \times \tau_{\text{wave}}$ where $\tau_{\text{wave}} = 2\pi/\Omega$, corresponding to $N_{\text{iter}} \cong 2.3 \times 10^6$): a) $\eta = 1 \times 10^{-5}$ (no PAS), b) $\eta \cong 10^{-4}$, c) $\eta = 8.5 \times 10^{-5}$, d) $\eta \cong 7 \times 10^{-5}$, e) $\eta \cong 7.1 \times 10^{-5}$, f) $\eta \cong 7.2 \times 10^{-5}$.

rotates without changing its shape such that an illusion of a solid structure is created.

For some values of η , in particular, converged PAS display (Figs. 5(b) and 5(c)) a *regular* shape with “lobes” (appearing as *petals* in the projection of the PAS on the xy plane) equally spaced in the azimuthal direction (with a resulting behavior similar to that typically observed for Marangoni flow in liquid bridges with a single toroidal roll^{20–24}). A range of values of η , however, exists (see, e.g., Fig. 5(d)) for which PAS formed by the combination of branches pertaining to distinct rolls are possible.

No definition is perfect, and it is hard to disentangle a definition from a property, but the following categorization captures the essential aspects of the observed phenomena. Three categories of possible PAS, in fact, can be defined on the basis of the present observations: (i) *regular* PAS lines given by the collective behavior of particles all attracted by a closed path located on a single toroidal roll (as an example

Fig. 5(b) shows PAS “locked” on the external roll); (ii) PAS pattern given by the *independent* existence of regular closed lines formed on different rolls (Fig. 5(c)); (iii) *irregular* closed lines due to the combination of portions of paths pertaining to class (ii) (Figs. 5(d)–5(f)). In particular, the number of possible variants for this last case has been found to be very high (with even minute variations of the η parameter in the range $5 \times 10^{-5} < \eta < 10^{-4}$ producing a myriad of different patterns and irregular shapes such as those shown in Figs. 5(d)–5(f)). Given the observed peculiar behavior, such a class of irregular geometric objects has been further investigated by repeating several times the same numerical simulation at a fixed value of η for arbitrarily changing initial positions of the solid particles (so to assess the nature of the observed multiplicity of solutions).

These simulations have confirmed that the topology of the PAS after the typical time (τ_{PAS}) required for their formation (according to the present simulations, approximately two

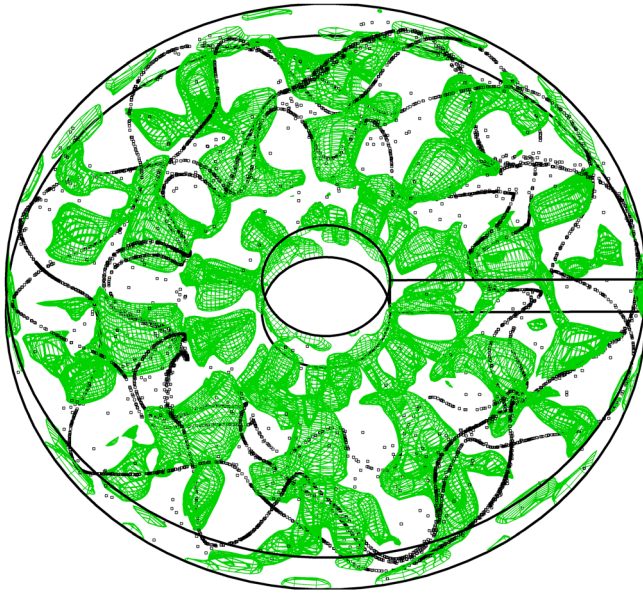


FIG. 6. PAS lines and isosurfaces of fluid (local) angular velocity for $\Theta_{\text{fluid}} \cong 5.4$ (PAS lines stay attached to the isosurfaces of fluid local angular velocity where $\Theta_{\text{fluid}} = \Omega$ as predicted by the so-called phase-locking theory).

times the overall wave revolution period, i.e., $\tau_{\text{PAS}} \cong 2 \times \tau_{\text{wave}}$ where $\tau_{\text{wave}} = 2\pi/\Omega$, which corresponds to a number of iterations $N_{\text{iter}} = \tau_{\text{PAS}}/\Delta t \cong 2.3 \times 10^6$) does not depend significantly on the particle initial positions, being essentially a function of η (thereby providing evidence for the strong sensitivity of such objects (attractors) to particle inertia).

The PAS shapes shown in Figs. 5(b), 5(c), 5(e), and 5(f) were found to be stable with a further increase of time ($N_{\text{iter}} = 5 \times \tau_{\text{PAS}}/\Delta t \cong 1.1 \times 10^7$) with the fluid surrounding the PAS being progressively depleted of particles as time passes (particles being “captured” by PAS). Interestingly, however, in some cases it was not possible to achieve a fully converged behavior even increasing the computational time by a factor 25 ($N_{\text{iter}} \cong 6 \times 10^7$, corresponding to 60 days of simulation on a computer equipped with an Intel Core Duo CPU E7500). A clear example of such a circumstance is shown in Fig. 5(d).

The number of particles fluctuating in a given neighborhood of the PAS clearly visible in this figure was found to remain almost constant (less than 5% variation) over the extended period simulated ($2.4 \times 10^6 < N_{\text{iter}} < 6 \times 10^7$).

In general, given intrinsic limitations of the approach used (direct numerical solution of the Navier-Stokes equation, very high computational time, etc.), it was not possible to assess the behavior of the system in the ideal limit as the time $t \rightarrow \infty$. Section IV, however, is devoted to elaborate specific considerations about the possible existence of a *general overarching attractor* governing all such dynamics and about the reason why a swarm of fluctuating particles not fully attracted by PAS may exist in some cases.

IV. DISCUSSION

Starting point of our discussion is the simple realization that despite the richness of shapes displayed by irregular PAS (class iii), the resulting onedimensional structures manifest a

very high, *but discrete*, number of variants (all produced by combination of branches related to regular paths).

This property provides the hint for the existence of a possible general overarching attractor/principle (not depending on particle properties, being rather an intrinsic “topological” property of the base velocity field).

Figure 6 is a view of PAS in which they have been plotted together with the isosurfaces of fluid (local) angular velocity $\Theta_{\text{fluid}} = \zeta_z/2$, where ζ_z is the axial component of vorticity. This view is particularly meaningful if we recall that, in general, the two components of vorticity $\underline{\zeta} = \nabla \wedge \underline{V}$ in the azimuthal, and axial directions

$$\zeta_\varphi = \left(\frac{\partial V_r}{\partial z} - \frac{\partial V_z}{\partial r} \right), \quad (5a)$$

$$\zeta_z = \frac{1}{r} \left[\frac{\partial}{\partial r} (r V_\varphi) - \frac{\partial V_r}{\partial \varphi} \right], \quad (5b)$$

can be regarded, respectively, as a measure of the strength of the basic toroidal roll(s) (ζ_φ) and departure from the axisymmetric state (ζ_z).

The latter contribution, in fact, is zero if it is evaluated in the axisymmetric state (the aforementioned target pattern with circular concentric rolls), but it is nonzero in a 3D state where, more specifically, its half ($\zeta_z/2$) can be regarded as a measure of the local average angular velocity (spin) of the considered fluid element about the vertical direction (see, e.g., Ref. 38).

Most remarkably, Figure 6 makes evident that PAS lines tend to stay attached everywhere to the isosurfaces $\Theta_{\text{fluid}} = \Omega$ (there is a strong geometrical correlation between such isosurfaces and the PAS; this figure has been obtained for $\eta = 8.5 \times 10^{-5}$, the property of PAS of staying attached everywhere to the isosurface, however, has been verified for all the considered values of this parameter), thereby lending further credence and validation to the theory originally elaborated by Schwabe *et al.*²³ and Pushkin *et al.*²⁹ for Marangoni flow, by which PAS occurs because the “turnover particle motion” becomes synchronized with the rotating wave oscillations.

Extremely tiny differences in the initial value used for η lead to significant variations in the calculations (in terms of shape of resulting PAS), an important restriction, however, being represented by the property of PAS of staying attached to the general overarching attractor given by the set of points satisfying the condition $\Theta_{\text{fluid}} = \Omega$.

At this stage, the existence of a limited number of particles fluctuating in a given neighborhood of the PAS for certain values of the inertia parameter may be “seen” as the effect of the attractive action exerted on them by distinct rolls via the phase-locking mechanism. Under a similar perspective, this behavior may be seen as a consequence of the (co)existence of distinct possible PAS at close values of the inertia parameter, i.e., as a natural consequence of the multiplicity of solutions, which of the PAS in RB convection is the most striking feature.

In other words, specific values of η may exist at which the attractive action exerted on particles by two distinct paths

(both satisfying the condition $\Theta_{\text{fluid}} = \Omega$, see Fig. 6) may be comparable, thus, preventing all particles from being fully captured by a single path.

The possible competition between distinct solutions existing at close values of the control parameter is not a new fact in the dynamics of nonlinear systems (in general), and in fluid-dynamics (in particular); the interested reader is referred to, e.g., the excellent studies about the multiplicity of solutions and the so-called “bistability” problem in thermogravitational convection by Refs. 39–42. These fascinating aspects (which are also common to other disciplines and fields^{43–46}) certainly deserve attention also in the case of PAS dynamics and it will be the subject of future studies.

V. CONCLUSIONS

The main conclusion of this analysis can be summarized as follows:

- PAS can emerge in RB convection provided specific conditions are established (which are the existence of at least one roll with toroidal structure and a disturbance traveling in the azimuthal direction having the characteristics of a wave; conditions that seem to be satisfied only for $\text{Pr} \cong 1$ in a region of the space of parameters, where the so-called OS mode of the Busse balloon occurs);
- An intrinsic feature of PAS patterns in RB flow is their variety (not observed in Marangoni flow);
- The richness of PAS shapes should be regarded as the result of the tendency of particles to select one of the several possible “attractive” paths according to their inertia;
- The sea of potential paths and their tortuosity are supported by the “granularity” of the surfaces satisfying the condition for phase locking $\Theta_{\text{fluid}} = \Omega$ (which makes possible the formation of PAS) in the OS state (Fig. 6).

The resulting mathematical relationship between particle axial vorticity and the characteristic phase velocity of propagation of the disturbance, and its application to cases which have nothing to do with Marangoni convection, in its broadest sense, provides a general theory to characterize the properties of all PAS phenomena produced by distinct types of flows.

To some extent the criterion identified here ($\Theta_{\text{fluid}} = \Omega$) may simplify the considered subject by abstracting from specific cases (Marangoni flow in geometries with free surfaces and RB convection in geometries entirely delimited by solid walls) features which are essential in the description of the general phenomenon of PAS in other circumstances (not necessarily related to these examples), thereby allowing the phase-locking theory for PAS formation^{23,24,29} to spread from its initial heartland of surface-tension-driven flows and related disciplines to a more general (perhaps universal) context.

With specific regard to RB convection, moreover, the identification of a new “family” of attractors, together with the related intrinsic multiplicity and sensitivity to particle inertia, is of enormous conceptual significance. Indeed, it opens new fascinating (heretofore unexplored) perspectives in the study of this kind of convection in combination with

particle aggregation phenomena and related theories for pattern formation in a variety of fields [ranging, just to cite some examples, from mechanisms operating at very large scales (e.g., related to the initial stages of planet formation driven by the accumulation of small dust particles), to all small-scale technological applications which simply share the use of microfluidic devices to manipulate the transport of tiny particles].

ACKNOWLEDGMENTS

This work is supported by the Italian Space Agency (ASI) in the framework of the JEREMI (Japanese and European Research Experiment on Marangoni Instabilities) Project for the preparation and execution of an experiment onboard the International Space Station (ISS).

- ¹P. Bergé, Y. Pomeau, and C. Vidal, *Order Within Chaos-Towards a Deterministic Approach to Turbulence* (John Wiley, New York, USA, 1984).
- ²W. Pesch, “Complex spatiotemporal convection patterns,” *Chaos* **6**(3), 348 (1996).
- ³F.H. Busse and R.M. Clever, “Asymmetric squares as an attracting set in Rayleigh-Bénard convection,” *Phys. Rev. Lett.* **81**, 341 (1998).
- ⁴H. Riecke and S. Madruga, “Geometric diagnostics of complex patterns: Spiral defect chaos,” *Chaos* **16**, 013125 (2006); D. A. Egolf, I. V. Melnikov, W. Pesch, and R. E. Ecke, “Mechanisms of extensive spatiotemporal chaos in Rayleigh-Bénard convection,” *Nature* **404**, 733 (2000); B. A. Malomed and A. A. Nepomnyashchy, “Coexistence of patterns on a ramp of overcriticality,” *Phys. Lett. A* **244**(1–3), 92 (1998).
- ⁵F. H. Busse and R. M. Clever, “Instabilities of convection rolls in a fluid of moderate Prandtl number,” *J. Fluid Mech.* **91**, 319 (1979).
- ⁶R. M. Clever and F. H. Busse, “Three-dimensional knot convection in a layer heated from below,” *J. Fluid Mech.* **198**, 345 (1989); R. M. Clever and F. H. Busse, “Steady and oscillatory bimodal convection,” *J. Fluid Mech.* **271**, 103 (1994).
- ⁷M. Lappa, *Thermal Convection: Patterns, Evolution and Stability* (John Wiley & Sons, Chichester, England, 2010).
- ⁸C. Bizon, J. Werne, A. A. Predtechensky, K. Julien, W. D. McCormick, J. B. Swift, and H. L. Swinney, “Plume dynamics in quasi-2D turbulent convection,” *Chaos* **7**(1), 107 (1997).
- ⁹A. P. Vincent and D. A. Yuen, “Plumes and waves in two-dimensional turbulent thermal convection,” *Phys. Rev. E* **60**(3), 2957 (1999).
- ¹⁰S. Childress, “Eulerian mean flow from an instability of convective plumes,” *Chaos* **10**(1), 28 (2000).
- ¹¹M. Lappa, “Some considerations about the symmetry and evolution of chaotic Rayleigh-Bénard convection: The flywheel mechanism and the “wind” of turbulence,” *C. R. Méc.* **339**, 563 (2011).
- ¹²N. Raju and E. Meiburg, “The accumulation and dispersion of heavy particles in forced two-dimensional mixing layers. Part 2: The effect of gravity,” *Phys. Fluids* **7**, 1241 (1995).
- ¹³M. R. Maxey, B. K. Patel, E. J. Chang, and L.-P. Wang, “Simulations of dispersed turbulent multiphase flow,” *Fluid Dyn. Res.* **20**(1–6), 143 (1997).
- ¹⁴E. Balkovsky, G. Falkovich, and A. Fouxon, “Intermittent distribution of inertial particles in turbulent flows,” *Phys. Rev. Lett.* **86**, 2790 (2001).
- ¹⁵C. Pasquero, A. Provenzale, and E. A. Spiegel, “Suspension and fall of heavy particles in random two-dimensional flow,” *Phys. Rev. Lett.* **91**, 054502 (2003).
- ¹⁶A. Esmaeili, “Phase distribution of bubbly flows under terrestrial and microgravity conditions,” *Fluid Dyn. Mater. Process.* **1**(1), 63 (2005); M. Lappa, “Coalescence and non-coalescence phenomena in multi-material problems and dispersed multiphase flows: Part 1, a critical review of theories,” *ibid.* **1**, 201 (2005); “Coalescence and non-coalescence phenomena in multi-material problems and dispersed multiphase flows: Part 2, a critical review of CFD approaches,” *ibid.* **1**, 213 (2005).
- ¹⁷R. D. Vilela and A. E. Motter, “Can aerosols be trapped in open flows?,” *Phys. Rev. Lett.* **99**, 264101 (2007).
- ¹⁸D. Di Carlo, J. F. Edd, K. J. Humphry, H.A. Stone, and M. Toner, “Particle segregation and dynamics in confined flows,” *Phys. Rev. Lett.* **102**, 094503 (2009).

- ¹⁹E. W. Saw, R. A. Shaw, S. Ayyalasomayajula, P. Y. Chuang, and A. Gylfason, "Inertial clustering of particles in high-Reynolds-number turbulence," *Phys. Rev. Lett.* **100**, 214501 (2008).
- ²⁰D. Schwabe, P. Hintz, and S. Frank, "New features of thermocapillary convection in floating zones revealed by tracer particle accumulation structures," *Microgravity Sci. Tech.* **9**, 163 (1996).
- ²¹I. Ueno, S. Tanaka, and H. Kawamura, "Oscillatory and chaotic thermocapillary convection in a half-zone liquid bridge," *Phys. Fluids* **15**(2), 408 (2003); "Various flow patterns in thermocapillary convection in half-zone liquid bridge of high Prandtl number fluid," *Adv. Space Res.* **32**(2), 143 (2003).
- ²²D. Schwabe, A. I. Mizev, S. Tanaka, and H. Kawamura, "Particle accumulation structures in time-dependent thermocapillary flow in a liquid bridge under microgravity," *Microgravity Sci. Tech.* **18**(3–4), 117 (2006); S. Tanaka, H. Kawamura, I. Ueno, and D. Schwabe, "Flow structure and dynamic particle accumulation in thermocapillary convection in a liquid bridge," *Phys. Fluids* **18**, 067103 (2006).
- ²³D. Schwabe, A. I. Mizev, M. Udhayasankar, and S. Tanaka, "Formation of dynamic particle accumulation structures in oscillatory thermocapillary flow in liquid bridges," *Phys. Fluids* **19**(7), 072102 (2007).
- ²⁴M. Lappa, "Assessment of the role of axial vorticity in the formation of particle accumulation structures in supercritical Marangoni and hybrid thermocapillary-rotation-driven flows," *Phys. Fluids* **25**, 012101 (2013).
- ²⁵E. Hofmann and H. C. Kuhlmann, "Particle accumulation on periodic orbits by repeated free surface collisions," *Phys. Fluids* **23**, 072106 (2011).
- ²⁶M. R. Maxey and J. J. Riley, "Equation of motion for a small rigid sphere in a nonuniform flow," *Phys. Fluids* **26**, 883 (1983).
- ²⁷M. R. Maxey, "The gravitational settling of aerosol particles in homogeneous turbulence and random flow fields," *J. Fluid Mech.* **174**, 441–465 (1987); G. Haller and T. Sapsis, "Where do inertial particles go in fluid flows?," *Physica D* **237**(5), 573 (2008).
- ²⁸T. Sapsis and G. Haller, "Clustering criterion for inertial particles in two-dimensional time-periodic and three-dimensional steady flows," *Chaos* **20**, 017515 (2010).
- ²⁹D. Pushkin, D. Melnikov, and V. Shevtsova, "Ordering of small particles in one-dimensional coherent structures by time-periodic flows," *Phys. Rev. Lett.* **106**, 234501 (2011).
- ³⁰D. Schwabe and A. I. Mizev, "Particles of different density in thermocapillary liquid bridges under the action of travelling and standing hydrothermal waves," *Eur. Phys. J. Special Topics* **192**, 13 (2011).
- ³¹F. H. Busse and R. M. Clever, "An asymptotic model of two-dimensional convection in the limit of low Prandtl number," *J. Fluid Mech.* **102**, 75 (1981).
- ³²R. M. Clever and F. H. Busse, "Low Prandtl number convection in a layer heated from below," *J. Fluid Mech.* **102**, 61 (1981); R. M. Clever and F. H. Busse, "Nonlinear oscillatory convection," *ibid.* **176**, 403 (1987).
- ³³V. Croquette, "Convective pattern dynamics at low Prandtl number: Part II," *Contemp. Phys.* **30**, 153 (1989).
- ³⁴M. Lappa, *Fluids, Materials and Microgravity: Numerical Techniques and Insights into the Physics* (Elsevier Science, Oxford, England, 2004).
- ³⁵M. Lappa, "Three-dimensional numerical simulation of Marangoni flow instabilities in floating zones laterally heated by an equatorial ring," *Phys. Fluids* **15**, 776 (2003); "Combined effect of volume and gravity on the three-dimensional flow instability in non-cylindrical floating zones heated by an equatorial ring," *ibid.* **16**(2), 331 (2004); M. Lappa, R. Savino, and R. Monti, "Influence of buoyancy forces on Marangoni flow instabilities in liquid bridges," *Int. J. Numer. Methods Heat Fluid Flow* **10**(7), 721 (2000).
- ³⁶D. Melnikov, D. Pushkin, and V. Shevtsova, "Accumulation of particles in time-dependent thermocapillary flow in a liquid bridge. Modeling of experiments," *Eur. Phys. J. Special Topics* **192**, 29 (2011).
- ³⁷K. A. Atkinson, *An Introduction to Numerical Analysis*, 2nd ed. (John Wiley & Sons, New York, 1989).
- ³⁸M. Lappa, *Rotating Thermal Flows in Natural and Industrial Processes* (John Wiley & Sons, Chichester, England, 2012).
- ³⁹B. Hof, G. J. Lucas, and T. Mullin, "Flow state multiplicity in convection," *Phys. Fluids* **11**, 2815 (1999).
- ⁴⁰A. Yu. Gelfgat, P. Z. Bar-Yoseph, and A. L. Yarin, "Stability of multiple steady states of convection in laterally heated cavities," *J. Fluid Mech.* **388**, 315 (1999).
- ⁴¹Y. Hu, R. Ecke, and G. Ahlers, "Transition to spiral-defect chaos in low Prandtl number convection," *Phys. Rev. Lett.* **74**, 391 (1995).
- ⁴²R. V. Cakmur, D. A. Egolf, B. B. Plapp, and E. Bodenschatz, "Bistability and competition of spatiotemporal chaotic and fixed point attractors in Rayleigh-Bénard convection," *Phys. Rev. Lett.* **79**(10), 1853 (1997).
- ⁴³M. Lappa, "Thermal convection and related instabilities in models of crystal growth from the melt on earth and in microgravity: Past history and current status," *Cryst. Res. Technol.* **40**(6), 531 (2005); M. Lappa and R. Savino, "3D analysis of crystal/melt interface shape and Marangoni flow instability in solidifying liquid bridges," *J. Comput. Phys.* **180**(2), 751 (2002).
- ⁴⁴M. Lappa, "Secondary and oscillatory gravitational instabilities in canonical three-dimensional models of crystal growth from the melt, Part 1: Rayleigh-Bénard systems," *C. R. Mec.* **335**(5–6), 253 (2007); "Part 2: Lateral heating and the Hadley circulation," *ibid.* **335**(5–6), 261 (2007).
- ⁴⁵M. Lappa, D. Castagnolo, and L. Carotenuto, "Sensitivity of the nonlinear dynamics of Lysozyme 'Liesegang Rings' to small asymmetries," *Physica A* **314**/1–4, 623 (2002).
- ⁴⁶L. Carotenuto, C. Piccolo, D. Castagnolo, M. Lappa, and J. M. García-Ruiz, "Experimental observations and numerical modelling of diffusion-driven crystallisation processes," *Acta Crystallogr.* **58**, 1628 (2002); M. Lappa, "A theoretical and numerical multiscale framework for the analysis of pattern formation in protein crystal engineering," *Int. J. Multiscale Comp. Eng.* **9**(2), 149 (2011).